Journal of the Serbian Chemical Society
JSCS-info@shd.org.rs • www.shd.org.rs/JSCS
J. Serb. Chem. Soc. *84* (11) 1221–1234 (2019)
JSCS–5259
UDC 546.47'711+544.654.2:620.193+544.6.076.32
Original scientific paper

The importance of using hydrogen evolution inhibitor during the Zn and Zn–Mn electrodeposition from ethaline

MIHAEL BUČKO[1#], MILORAD V. TOMIĆ[2], MIODRAG MAKSIMOVIĆ[3] and JELENA B. BAJAT[3*#]

[1]University of Defense, Military Academy, 33 Pavla Jurišića Šturma St, 11000 Belgrade, Serbia, [2]University of East Sarajevo, Faculty of Technology Zvornik, Republic of Srpska, B&H and [3]Faculty of Technology and Metallurgy, University of Belgrade, P.O .Box 3503, 11120 Belgrade, Serbia

(Received 18 July, revised 16 August, accepted 19 August 2019)

Abstract: Cyclic voltammetry was used for the characterization of zinc electrodeposition on steel from ethaline deep eutectic solution (1:2 choline chloride:ethylene glycol). The influence of 4-hydroxy-benzaldehyde (HBA) as an additive was analyzed. It was shown that hydrogen evolution is inhibited in the presence of HBA and further significantly retarded upon addition of Zn^{2+} to the solution containing HBA. The cathodic peak for Zn^{2+} reduction in this type of ionic liquid (ethaline+HBA+Zn^{2+}) resembles the zinc reduction in aqueous solution. The corrosion resistance of Zn coatings deposited at different current densities was evaluated by electrochemical methods, *i.e.*, polarization measurements and electrochemical impedance spectroscopy in 3 % NaCl solution. The possibility of Zn–Mn alloy deposition from ethaline deep eutectic solvent was investigated for the first time. In addition, the corrosion stability of these alloy coatings was analyzed and compared to the stability of bare Zn coatings. It was shown that the optimum deposition current density for both Zn and Zn–Mn coatings with increased corrosion stability from ethaline + HBA electrolyte is 5 mA cm^{-2}.

Keywords: deep eutectic solvents; electrodeposition; hydrogen evolution; coatings; corrosion.

INTRODUCTION

Deep eutectic solvent (DES) may be defined as a liquid consisting of two or three cheap and safe components that are capable of self-association, usually through hydrogen bond interactions to form an eutectic mixture.[1] These solvents show similar physico-chemical properties to the traditionally used ionic liquids

*Corresponding author. E-mail: jela@tmf.bg.ac.rs
Serbian Chemical Society active member.
https://doi.org/10.2298/JSC190718084B
●Dedicated to the memory of Prof. Dr Konstantin Popov, our distinguished Professor and a leading expert in the field of metal electrodeposition.

but are cheaper and environmentally friendlier. As a result, DESs are nowadays being applied in many fields of research, for example in electrochemistry, material chemistry, dissolution and extraction processes, catalysis, organic synthesis, *etc*.[1] Due to the fact that many DES types possess a wide electrochemical window, good solvation ability for various metal salts, good ionic conductivity, and environmental friendliness, they have also found application in the electroplating industry.[1] To date, the list of metals and alloys that have been successfully electrodeposited from DESs is very long. A recent review on this topic includes, but is not limited to, Ni, Cr, Zn, Al, Cu, Ag, and Mg metal coatings, as well as alloys for anticorrosion protection (Zn–Ni, Zn–Sn, *etc.*), magnetic alloys (Ni–Co, Ni–Fe–Cr, Sm–Co, *etc*.), semiconductors and photovoltaic alloys (In–Ga, $CuGaSe_2$), and alloys for electrocatalytic application (Ni–Co–Sn, Co–Pt).[2]

Our group focuses research on Zn–Mn alloy electroplating as a corrosion resistant coating on steel, from aqueous solutions,[3] but we also reported the electrodeposition process of Zn–Mn alloy from deep eutectic mixture of choline chloride and urea, with trade name reline.[4] The motivation for using DES in Zn–Mn electroplating is the fact that water baths suffer from instability, low current efficiency or poor deposit morphology due to the hydrogen evolution reaction.[5] A literature search evidenced that only a few research groups have tackled the possibility of Zn–Mn electrodeposition from choline-based deep eutectic solvents: reline with boric acid as an additive was used for electrodepositing Zn–Mn on copper,[6,7] while acetylcholine chloride-urea eutectic mixture was employed for Zn–Mn electroplating from the leached liquors of spent alkaline batteries.[8]

Besides reline, the second most successfully characterized and the most often cited DES in the last two decades is ethaline (a eutectic mixture of choline chloride and ethylene glycol). Yet, to the best of our knowledge, ethaline has hitherto not been applied in Zn–Mn electrodeposition, although it was reported as an electrolyte for electroplating of other Zn alloys, two examples of which are Zn–Sn,[9] and Zn–Ni alloy.[10]

The possibility of Zn–Mn alloy deposition from ethaline deep eutectic solvent has been investigated for the first time. Since we are not aware that there is any report in the literature on the deposition of Zn–Mn coatings from ethaline, the electrodeposition and corrosion stability of these Zn alloy coatings was examined and compared to the behaviour of Zn coatings. The Zn–Mn alloy coatings are of interest for electrodeposition from ionic liquids due to the very negative Mn standard electrode potential. Namely, Mn electrodeposition in aqueous solutions is accompanied with massive hydrogen evolution, resulting in very low current efficiencies. It has been reported that Zn–Mn coatings offer excellent steel corrosion protection due to the passive films of corrosion products that are formed in corrosive environments.

The influence of 4-hydroxy-benzaldehyde (HBA) as an additive was analyzed. HBA is known as an inhibitor of hydrogen evolution, and hence it could have a two-fold action, *i.e.*, an increase of the current efficiency by retarding hydrogen evolution and, consequently, suppression of hydroxide formation.[3]

EXPERIMENTAL

Electrodeposition of Zn and Zn–Mn alloy coatings

Choline chloride (Aldrich, 99 %), ethylene glycol (Aldrich, 99 %), zinc chloride (Aldrich, >98 %), manganese(II) chloride ($MnCl_2 \cdot 4H_2O$) (Aldrich, >99 %) and 4-hydroxy-benzaldehyde were used as obtained. The eutectic mixture was formed at 25 °C by stirring a 1:2 mole ratio mixture of dried choline chloride and the ethylene glycol hydrogen bond donor until a homogeneous colourless liquid was observed. The plating electrolytes were formed by adding 5.0 g dm^{-3} HBA, 0.40 mol dm^{-3} $ZnCl_2$ and 0.10 mol dm^{-3} $MnCl_2 \cdot 4H_2O$ to the deep eutectic solvent and stirring the mixture at 25 °C until homogeneous electrolytes were obtained.

The electrodeposition of Zn and Zn–Mn coatings was realised at 25 °C using a steel working electrode (20 mm×20 mm×0.25 mm) and a high purity zinc counter electrode. The coatings were deposited galvanostatically, using a potentiostat PAR M273A, at 1, 3, 5, 8 or 12 mA cm^{-2}. The electrodeposition time was adjusted to obtain deposits of the same thickness (5 μm) by maintaining the same electrodeposition charge density in each experiment. The steel electrode was mechanically prepared using abrasive emery papers down to 1200 grit, degreased in a saturated solution of NaOH in ethanol, pickled with 2 mol dm^{-3} HCl for 30 s, and finally rinsed with distilled water, acetone and dried in air by a fan. After electrodeposition, the samples were cleaned with acetone and dried in air by a fan.

Electrochemical measurements

Voltammetric experiments were performed by cyclic voltammetry at 1.0 mV s^{-1} between –650 and –1550 mV *vs*. SCE, using a potentiostat ZRA Reference 600, Gamry Instruments.

The corrosion stability of the Zn and Zn–Mn coatings was determined by electrochemical impedance spectroscopy (EIS) and polarization measurements in an aerated 3 wt. % NaCl solution. A classic three-electrode cell with a platinum mesh as counter electrode, coated steel (1 cm^2) as the working electrode and a saturated calomel electrode as reference was used. The EIS measurements were obtained at the open circuit potential (OCP) in a frequency range of 100 kHz–0.01 Hz, using a 10 mV amplitude perturbation. In the polarization measurements, a potential sweep rate of 1.0 mV s^{-1} was applied starting from –250 mV *vs*. OCP and ending at 250 mV *vs*. OCP, after achieving a constant OCP (30 min). The corrosion rates of the deposited coatings were determined using extrapolation of anodic polarization curves to the open circuit potential (OCP).

RESULTS AND DISCUSSION

Calculation of surface pH during the electrodeposition process

During electrodeposition of an electronegative metal, the hydrogen evolution reaction occurs in parallel with metal electroreduction, when the electrode potential is sufficiently negative for this parasitic process to occur. In addition to the decrease in current efficiency, the other drawback of hydrogen evolution may be the formation of unwanted hydroxides at the electrode surface, in the case that a sufficient concentration of hydroxyl ions is attained.[11]

It is well known that choline chloride based DESs are extremely hygroscopic mixtures, so they contain some percent of water, which is electroreduced at the cathode during the electrodeposition, by the same mechanism as in aqueous electrolytes.[12,13] Therefore, it would be interesting to calculate the pH change in the vicinity of the cathode during the electrodeposition process, and to compare the results for DESs with those for an aqueous solution.

The concentration of OH^- ion in the diffusion layer during water electrolysis may be calculated according to Eq. (1):

$$c(OH^-) = c(OH^-)_1 + c(OH^-)_0 - c(OH^-)_2 \quad (1)$$

where the concentration value $c(OH^-)_1$ is the concentration of hydroxyl ion in the diffusion layer, produced in reaction (2):

$$2H_2O + 2e^- = H_2 + 2OH^- \quad (2)$$

According to the literature,[14] the time dependence of the average concentration of OH^- in the diffusion layer, generated in reaction (2), may be estimated using simple model, Eq. (3):

$$c\left(OH^-\right)_1(\tau) = \frac{0.274\,j}{nF\sqrt{D(OH^-)}}\sqrt{\tau} \quad (3)$$

where $D(OH^-)$ is the diffusion coefficient of the hydroxyl ion, and j is the current density related to water electrolysis (reaction (2)) and 0.247 is a constant (a detailed calculation of Eq. (3) is presented in the literature[14]).

The value $c(OH^-)_0$ is the bulk concentration of hydroxyl ion, represented as:

$$c(OH^-)_0 = \frac{K_w}{10^{-pH}} \quad (4)$$

Finally, the last term in Eq. (1), $c(OH^-)_2$, is the amount of hydroxyl ions, which diminishes in the reaction with hydrogen protons diffusing from the bulk solution. Namely, the diffusion coefficient of hydrogen proton is higher than that of the OH^- and hence, the concentration of OH^-, which decreases in the reaction with hydrogen protons diffusing from the bulk solution, is proportional to the ratio of the diffusion coefficients of the two species:

$$c(OH^-)_2 = \frac{D(H^+)}{D(OH^-)}10^{-pH} \quad (5)$$

Equation (1) was used to calculate the near-cathode pH change during the electrodeposition process, in pH neutral aqueous solution and in two choline chloride based deep eutectic solvents, *i.e.*, ethaline, and reline, which are mixtures of choline chloride–ethylene glycol and choline chloride–urea, respectively. It was assumed for the sake of simplicity that the water electrolysis occurs at a

current density of 1 μA cm^{-2}. This value was chosen arbitrarily, as a negligible value compared to the total current applied at the working electrode, if it is known that the deposition occurs at current densities in the range between 1 and 12 mA cm^{-2}, as will be discussed later in the text.

The parameters used in the calculation are given in Table I.

TABLE I. The diffusion coefficient and bulk pH values in water and DES, taken from the literature[15,16]

Parameter	Water	Ethaline	Reline
$D(OH^-)$ / 10^{-11} m^2 s^{-1}	530	6.0	0.2
$D(H^+)$ / 10^{-11} m^2 s^{-1}	931	6.0	0.2
pH of bulk electrolyte	7.00	6.41	8.61

Concerning the diffusivity coefficients for OH^- and H^+ in DES, we are not aware of explicit data in the literature. An NMR study showed that in both ethaline and reline,[17] the water molecule has higher diffusivity as compared to the hydrogen bond donor (ethylene glycol or urea) and the choline cation. As the water content in DES increased, the diffusivity of the hydrogen proton (measured by following with NMR the movement of the OH groups of the choline cation and the hydrogen bond donor) became significantly higher than that for the parent species, *i.e.*, the choline cation and hydrogen bond donor, denoting that diffusion of the hydrogen proton occurs through phenomena such as interaction/ /pairing/exchange between hydroxyl protons of different molecules,[17] similar phenomena that are used for the explanation of the high diffusivity of H^+ and OH^- in water solutions. However, in "dry" DES, *i.e.*, DES with a very low water content, this phenomenon was not detected.[17] Furthermore, the reported *D* values for all species (water, choline ion, hydrogen bond donor) in DES with even as much water as 10 wt. % were of the order of 10^{-11} m^2 s^{-1}. When the analogy with aqueous media is made, it is known that the *D* values for H^+ and OH^- in water are of the same order of magnitude as for ionic species of metals salts, as well as for water molecules themselves.[18] Bearing all these facts in mind, it seems reasonable to ascribe the *D* values for H^+ and OH^- in ethaline and reline as presented in Table I, which are, actually, the *D* values for water molecule in DES with a very low water content.[17]

The calculated values of pH change are presented in Fig. 1. Even when hydrogen evolution occurs at a current density as low as 1 μA cm^{-2}, it induces a significant pH change. Clearly, the pH rise is much higher in DESs compared to in water, due to the lower diffusivity of hydroxyl ion in these solvents. Consequently, there is higher probability that a hydroxide deposit is going to be formed at the working electrode in DES.

It should be born in mind that Eq. (1) is valid only until no hydrogen bubbles are formed at the cathode, because when gas is formed, it stirs the solution and so the mass transport of the hydroxyl ion is faster.

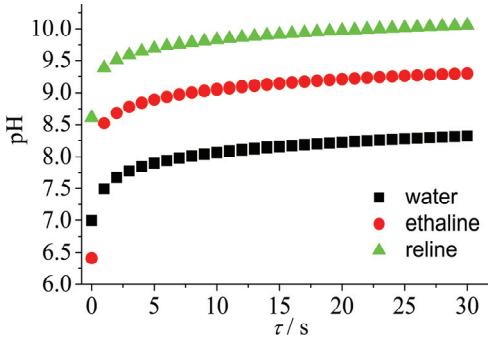

Fig. 1. The calculated pH change in the diffusion layer during the hydrogen evolution reaction, in three different media, using the parameters given in Table I.

One way of suppressing hydroxide formation is deposition in the presence of additives, such as hydrogen inhibitors. The influence of the additive 4-hydroxy--benzaldehyde in ethaline deep eutectic solution on the current efficiency and corrosion stability of electrodeposited Zn coatings will be further analyzed.

Cyclic voltammetry

Voltammetric studies were carried out in deep eutectic solutions, additive--free or containing HBA (Fig. 2).

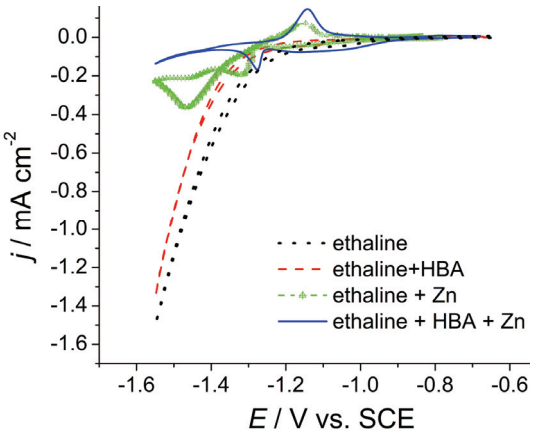

Fig. 2. Cyclic voltammograms in different DES electrolytes.

When the potential is scanned in the negative direction, starting from E_{ocp}, the onset of the cathodic current appears in a neat deep eutectic solvent at about –0.950 V (all potential in the text are referred *vs*. SCE) and at potentials below –1.15 V, there is a sharp increase in the cathodic current, pointing to electrolyte degradation, *i.e*., reduction of the hydroxyl groups in the ethylene glycol, choline

ions (Ch+) and/or hydrogen evolution originating from the presence of water in the DES.[19] When Zn^{2+} are introduced in ethaline, there is a cathodic peak negative to the potentials of electrolyte degradation, and another cathodic peak appeared during the backward anodic sweep. This behaviour has already been reported in the literature.[20–22] Namely, the mechanism of Zn electrodeposition from DESs has been explained based on tetrachlorozincates, $[ZnCl_4]^{2-}$, as the main zinc specie in a strong Lewis basic DES, such as ethaline. Due to the very negative reduction potential of tetrachlorozincate ions, direct zinc deposition from $[ZnCl_4]^{2-}$ occurs at a low rate (onward cathodic peak), but Zn deposition occurs also when $[ZnCl_{4-x}(RO)_x]^{2-}$ species are formed, *i.e.*, when one or two chloride ligands are replaced with ethoxy anion (RO^-) in the complex Zn ion (backward cathodic peak).[20]

In the DES containing HBA, the onset of the cathodic current is shifted to more negative values, –1.050 V, and a sharp increase in the cathodic current occurs at –1.3 V. This confirms the fact that similarly to in aqueous solutions,[3] the substituted benzaldehyde compound acts as a hydrogen evolution inhibitor also in a DES. The most important change was observed when Zn^{2+} were introduced in the electrolyte. Namely, the cathodic peak appeared already in the cathodic forward sweep at –1.28 V, signifying the reduction of Zn^{2+}, and there was also an anodic peak at –1.14 V related to the dissolution of the deposited zinc layer. This was followed by a significant decrease in the *j*–*E* slope at potential values negative to –1.28 V, pointing to great retardation of hydrogen evolution. The cathodic peak for Zn^{2+} reduction in this type of ionic liquid resembles that of the reduction in aqueous solution.

Current efficiency

The influence of the deposition current density on the current efficiency (CE, calculated based on the Faraday law), for Zn coatings, in the absence and presence of the additive HBA, is shown in Fig. 3. A very low current efficiency was obtained in the additive-free bath for all current densities (below 50 % for all deposits), indicating that some other reaction besides Zn deposition is occurring on the cathode. This could be either hydrogen evolution or reduction of some organic species from ethaline. Another phenomena was observed during electrodeposition, namely a large number of gas bubbles was present at the surface of the working electrode. Since there was no stirring, these bubbles remained at the electrode, inhibiting the process of coating deposition, and leading to low current efficiency. Since a zinc reduction peak in ethaline containing Zn^{2+} was observed after the decomposition of the bulk electrolyte (Fig. 2), it may be concluded that this parallel reduction reaction was already occurring before the onset of zinc deposition, *i.e.*, hydrogen had already been formed, resulting in a low current efficiency.

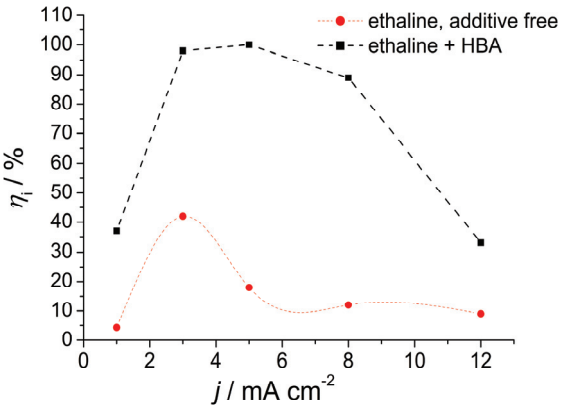

Fig. 3. The dependence of current efficiencies on the deposition current density for Zn deposition in the presence and absence of HBA additive.

When substituted benzaldehyde, as hydrogen evolution inhibitor, was added in ethaline, the current efficiency was considerably higher (Fig. 3), reaching even 100 % at intermediate deposition current densities. This behaviour could be expected based on the CVs in Fig. 2, since Zn reduction occurred before the bulk electrolysis, which was additionally shifted to more negative potentials.

In both plating baths, the CE increased with increasing deposition current density until after reaching a maximum at 3–5 mA cm^{-2}, it decreased again, which was especially pronounced in plating from the bath containing HBA. It should be noted that the coating deposited at 12 mA cm^{-2} from the HBA containing bath was powdery, dendritic and porous, so this could be the result of such a sudden CE drop. Therefore, higher deposition current densities were not examined. It seems that at current densities above 5 mA cm^{-2}, the electrode potential is so negative that HBA desorption occurs, leading to loss of its inhibiting effect, and to a fast hydrogen evolution process.

Corrosion study

The corrosion resistances of Zn-coatings electrodeposited at different current densities from ethaline with HBA additive were determined based on electrochemical measurements, *i.e.*, EIS and polarization measurements in 3 wt. % NaCl solutions. The potentiodynamic polarization curves obtained for all Zn samples are shown in Fig. 4.

The shape of all Tafel curves is the same, indicating diffusion controlled cathodic reaction and active dissolution in the anodic branch. Namely, scanning the potential in the negative direction in a range of ~200 mV from the open circuit potential, resulted in a small current density increase, which is typical behaviour for a diffusion controlled cathodic reaction of oxygen, when oxygen transport is limited due to its low solubility in the solution.[23,24] The small anodic polarization is characterized by substantial increase in current density, suggesting

active coating dissolution, typical for zinc corrosion in NaCl solution.[25] The Tafel slope is ≈40 mV dec^{-1}, as usually reported for zinc dissolution.[26] Given this behaviour and diffusion-controlled cathodic reaction, the corrosion current densities were evaluated by extrapolation of the anodic Tafel lines to the corrosion potential, E_{corr}, and the results are given in Table II.

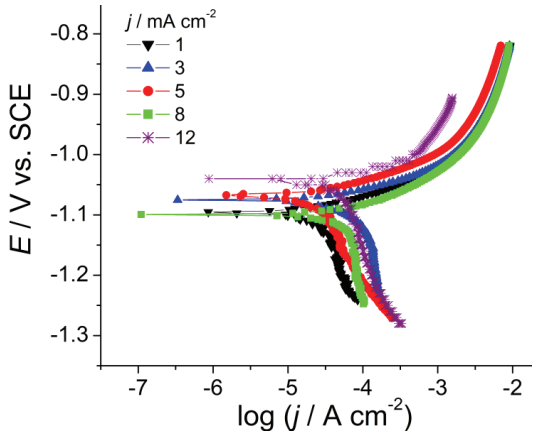

Fig. 4. Polarization curves in 3 % NaCl solution for Zn coatings deposited at different current densities from ethaline + HBA.

TABLE II. The dependence of corrosion parameters of the Zn-coatings on the electrodeposition current densities

j_{dep} / mA cm^{-2}	$-E_{corr}$ / V$_{SCE}$	J_{corr} / μA cm^{-2}
1	1.095	27.5
3	1.077	31.6
5	1.071	26.2
8	1.100	40.7
12	1.040	51.3

Lower corrosion current densities were measured for coatings deposited at lower current densities, the one at 5 mA cm^{-2} having the lowest value, *i.e.*, highest corrosion stability. Small alterations in corrosion potential, E_{corr}, depending on the deposition current density, could be observed. The coating deposited at 12 mA cm^{-2} showed the most positive E_{corr} value, which was probably a mixed value of the Zn-coating and steel substrate, since NaCl solution could easily reach the steel substrate through this porous coating.

The corrosion stability of Zn coatings electrodeposited from ethaline at different current densities was further studied by EIS at the open circuit potential. The recorded Nyquist plots are shown in Fig. 5.

The EIS spectra of the coatings deposited at lower current densities were characterized by two time constants, *i.e.*, one in the high-frequency range, related to the corrosion product film resistance, and another one at lower frequencies accounted for by corrosion processes at the coating interface underneath the cor-

rosion product film. The sum of both semicircle diameters was associated to the overall coating corrosion resistance, R_{corr}.[27] The largest overall impedance, shown as the sum of the two diameters, for coating deposited at 5 mA cm^{-2} points to its highest corrosion resistance, among the ones analyzed in this work. In the case of Zn coatings deposited at higher current densities, these two semicircles overlap and result in one time constant, indicating the R_{corr} values.

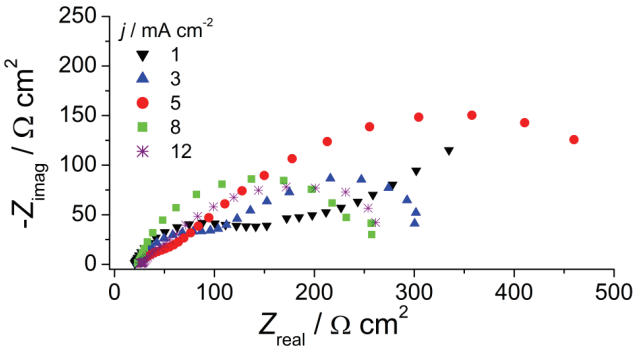

Fig. 5. Nyquist plots in 3 % NaCl solution for Zn coatings deposited from ethaline + HBA at different current densities.

The EIS spectra were fitted using equivalent electrical circuits shown in Fig. 6a and b, for plots characterized by one or two time constants, respectively. The elements of the circuits are: R_Ω – the electrolyte resistance; R_{po} – the electrolyte resistance in the pores of the corrosion product; R_{ct} –the charge transfer resistance and R_{corr} – the sum of the two resistances. Constant phase elements (CPE) were used instead of pure capacitances, where CPE_{po} represents the capacitance of porous corrosion product layer and CPE_{dl} is related to double layer capacitance.

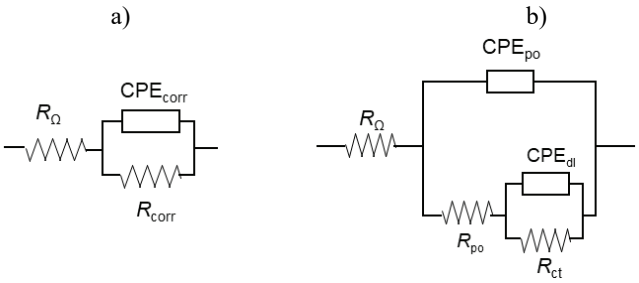

Fig. 6. Equivalent electrical circuit used for fitting of the impedance plots recorded at the Zn-coatings in 3 % NaCl.

The fitting of EIS experimental data provided R_{corr} values for Zn coatings and the results are shown in Fig. 7.

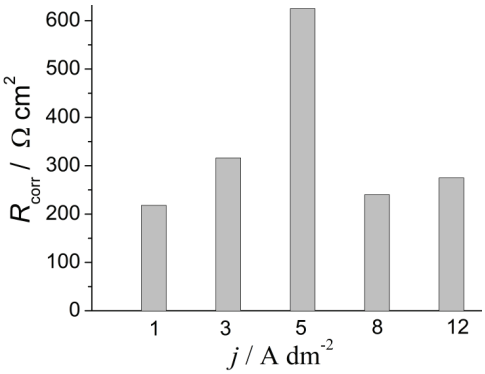

Fig. 7. The R_{corr} values for Zn-coatings deposited from ethaline + HBA at different current densities..

As can be seen from Figs. 5 and 7, the impedance of the coating deposited at 5 mA cm^{-2} was at least two times higher than the impedance of the other samples, pointing to its excellent corrosion stability. These results are in agreement with the ones given in Table II.

Furthermore, the electrodeposition and corrosion stability of Zn–Mn alloy coatings on steel were examined. Since the current efficiency was very low in Zn–Mn plating from ethaline + HBA, the deposition of the alloy coating was performed in two steps, *i.e.*, a thin bare Zn coating was deposited, which was afterwards used as a sub layer for Zn–Mn deposition. In this way, very high CEs were achieved and the overall thickness of the coating system was 5 μm.

Nyquist plots for Zn–Mn alloy coatings deposited from ethaline containing HBA at several current densities are shown in Fig. 8. The improvement of Zn coating corrosion stability is evident based on these plots. The R_{corr} values were even an order of magnitude higher than those for the pure Zn coatings. Namely, by fitting the experimental EIS data, the R_{corr} value for Zn–Mn coating deposited at 5 mA cm^{-2} was determined to be 3360 Ω cm^2. The R_{corr} values for Zn–Mn alloy coatings deposited at 3 and 8 mA cm^{-2} were smaller than this, *i.e*,. 1010 and 3190 Ω cm^2, respectively, but still significantly higher than the values determined for the Zn coatings.

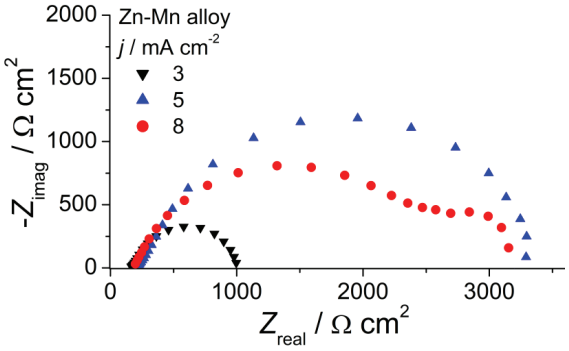

Fig. 8. Nyquist plots in 3 % NaCl solution for Zn–Mn coatings deposited at different current densities.

Hence, based on all the results, it can be concluded that Zn–Mn alloy coatings could be successfully deposited from ethaline in the presence of HBA. These coatings show excellent corrosion stability, and it was shown that 5 mA cm^{-2} was the optimal deposition current density.

CONCLUSIONS

This article reports the optimal conditions for the electrochemical deposition of Zn–Mn alloy coatings on steel substrates, from ethaline. Although there are reports on deposition of various Zn–alloys from ethaline, there is to the best of our knowledge no such report regarding Zn–Mn coatings. Based on the presented results, it may be concluded that both Zn and Zn–Mn deposition from additive-free ethaline occurs with very low current efficiency. For this reason, the hydrogen evolution inhibitor, *i.e.*, 4-hydroxy-benzaldehyde, was added to ethaline, and the effect was a significant increase in the current efficiency for Zn plating.

Concerning the Zn–Mn alloy, the current efficiency was low even with the addition of 4-hydroxy-benzaldehyde. Therefore, another approach was applied: a thin sub-layer of Zn was deposited on a bare steel surface, and then a thicker Zn–Mn coating was deposited, and by using these steps, a high current efficiency was achieved. The corrosion testing of both Zn and Zn–Mn coatings showed that the best properties were achieved at a deposition current density of 5 mA cm^{-2}.

Literature data on the bulk pH and diffusion coefficients of various species in reline and ethaline were used to calculate the expected pH change in the diffusion layer at the cathode during the electrodeposition process. As expected (due to the lower diffusivity), a much higher increase in the pH occurs in deep eutectic solvents, as compared to aqueous solution. This is another reason for using a hydrogen evolution inhibitor during electroplating from reline and ethaline.

Acknowledgements. This research was financed by the Ministry of Education, Science and Technological Development of the Republic of Serbia (Grant No. III 45019) and the Ministry for Scientific and Technological Development, Higher Education and Information Society of the Republic of Srpska (Grant No. 19/6-020/961-20/18).

ИЗВОД

ЗНАЧАЈ ПРИМЕНЕ ИНХИБИТОРА ИЗДВАЈАЊА ВОДОНИКА ПРИ ЕЛЕКТРОХЕМИЈСКОМ ТАЛОЖЕЊУ Zn И Zn–Mn ЛЕГУРЕ ИЗ ЕТАЛИНА

МИХАЕЛ БУЧКО[1], МИЛОРАД В. ТОМИЋ[2], МИОДРАГ МАКСИМОВИЋ[3] и ЈЕЛЕНА Б. БАЈАТ[3]

[1]Универзитет одбране, Војна академија, Павла Јуришића Штурма 33, 11000 Београд, [2]Универзитет у Источном Сарајеву, Технолошки факултет Зворник, Каракај бб, Република Српска и [3]Технолошко–металуршки факултет, Универзитет у Београду, Карнегијева 4, 11120 Београд

У овом раду је цикличном волтаметријом проучавано електрохемијско таложење превлака Zn и Zn–Mn легура из јонске течности, еталина (1:2 холин-хлорид:етиленгликол). Испитиван је утицај примене ароматичног алдехида (4-хидрокси-бензалдехида, HBA), као специфичног додатка. Показано је да је реакција издвајања водоника инхибирана у присуству HBA, и додатно успорена у присуству Zn^{2+}. Катодни пик редукције Zn^{2+} подсећа на редукцију цинка у воденим растворима. Корозиона стабилност пре-

влака цинка електрохемијски таложених различитим густинама струје је испитивана електрохемијским методама: поларизационим мерењима и спектроскопијом електрохемијске импеданције у раствору 3 % NaCl. Електрохемијско таложење Zn–Mn превлака из еталина је испитивано по први пут. Анализирана је корозиона отпорност ових легура и поређена са превлакама цинка. Показано је да је 5 mA cm^{-2} оптимална густина струје таложења, којом се добијају превлаке Zn и Zn–Mn легура повећане корозионе стабилности.

(Примљено 18. јула, ревидирано 16. августа, прихваћено 19. августа 2019)

REFERENCES

1. E. L. Smith, A. P. Abbott, K. S. Ryder, *Chem. Rev*. **114** (2014) 11060 (https://doi.org/10.1021/cr300162p)
2. R. Bernasconi, G. Panzeri, A. Accogli, F. Liberale, L. Nobili, L. Magagnin, *Electrodeposition from Deep Eutectic Solvents*, in *Progress and Developments in Ionic Liquids*, S. Handy, Ed., IntechOpen, Rijeka, 2017 (http://dx.doi.org/10.5772/64935)
3. M. Bučko, U. Lačnjevac, J. B. Bajat, *J. Serb. Chem. Soc*. **78** (2013) 1569 (https://doi.org/10.2298/JSC130118025B)
4. M. Bučko, D. Culliton, A. J. Betts, J. B. Bajat, *T. I. Met. Finish*. **95** (2017) 60 (http://dx.doi.org/10.1080/00202967.2017.1255412)
5. D. Sylla, C. Savall, M. Gadouleau, C. Rebere, J. Creus, Ph. Refait, *Surf. Coat. Technol*. **200** (2005) 2137 (https://doi.org/10.1016/j.surfcoat.2004.11.020)
6. P. P. Chung, P. A. Cantwell, G. D.Wilcox, G. W. Critchlow, *T. I. Met. Finish* **86** (2008) 211 (https://doi.org/10.1179/174591908X327572)
7. S. Fashu, C. Gu, J. Zhang, H. Zheng, X. Wang, J. Tu, *J. Mater. Eng. Perform*. **24** (2015) 434 (https://doi.org/10.1007/s11665-014-1248-5)
8. J. Aldana-González, A. Sampayo-Garrido, M. G. Montes de Oca-Yemha, W. Sánchez, M. T. Ramírez-Silva, E. M. Arce-Estrada, M. Romero-Romo, M. Palomar-Pardavé, *J. Electrochem. Soc*. **166** (2019) D199 (https://doi.org/10.1149/2.0761906jes)
9. N. M. Pereira, S. Salome, C. M. Pereira, A. Fernando Silva, *J. Appl. Electrochem*. **42** (2012) 561 (https://doi.org/10.1007/s10800-012-0431-3)
10. N. M. Pereira, C. M. Pereira, J. P. Araújo, A. Fernando Silva, *J. Electrochem. Soc*. **162** (2015) D325 (https://doi.org/10.1149/2.0161508jes)
11. L. Harris, *J. Electrochem. Soc*. **120** (1973) 1034 (https://doi.org/10.1149/1.2403622)
12. M. Bučko, S. Roy, P. Valverde-Armas, A. Onjia, A. C. Bastos, J. B. Bajat, *J. Electrochem. Soc*. **165** (2018) H1059 (https://doi.org/10.1149/2.0921816jes)
13. K. Haerens, E. Matthijs, K. Binnemans, B. Van der Bruggen, *Green Chem*. **11** (2009) 1357 (https://doi.org/10.1039/B906318H)
14. M. E. Tawfik, F. J. Diez, *Electrochim. Acta* **146** (2014) 792 (http://dx.doi.org/10.1016/j.electacta.2014.08.147)
15. S. H. Lee, J. C. Rasaiah, *J. Chem. Phys*. **135** (2011) 124505 (http://dx.doi.org/10.1063/1.3632990)
16. A. P. Abbott, S. S. Alabdullah, A. Y. Al-Murshedi, K. S. Ryder, *Faraday Discuss*. **206** (2018) 365 (https://doi.org/10.1039/C7FD00153C)
17. C. D'Agostino, L. F. Gladden, M. D. Mantle, A. P. Abbott, E. I. Ahmed, A. Y. Al-Murshedi, R. C. Harris, *Phys. Chem. Chem. Phys*. **17** (2015) 15297 (https://doi.org/10.1039/C5CP01493J)
18. P. Vanysek, *Ionic conductivity and diffusion at infinite dilution*, in *Handbook of Chemistry and Physics*, CRC Press, Boca Raton, FL, 1992/93

19. L. Vieira, R. Schennach, B. Gollas, *Electrochim. Acta* **197** (2016) 344 (http://dx.doi.org/10.1016/j.electacta.2015.11.030)
20. L. Vieira, A. H. Whitehead, B. Gollas, *J. Electrochem. Soc*. **161** (2014) D7 (http://dx.doi.org/10.1149/2.016401jes)
21. A. P. Abbott, J. C. Barron, G. Frisch, S. Gurman, K. S. Ryder, A. Fernando Silva, *Phys. Chem. Chem. Phys*. **13** (2011) 10224 (https://doi.org/10.1039/C0CP02244F)
22. Y. Lin, I. Sun, *Electrochim. Acta* **44** (1999) 2771 (https://doi.org/10.1016/S0013-4686(99)00003-1)
23. L. L. Shreir, R. A. Jarman, G. T. Burstein, Eds., *Corrosion*, 3rd ed., Butterworth-Heinemann, Oxford, 2000 (https://doi.org/10.1002/maco.19950460611)
24. R. G. Kelly, J. R. Scully, D. W. Shoesmith, R. G. Buchheit, in *Corrosion Science and Engineering*, Marcell Dekker, Inc., New York, 2002 (https://doi.org/10.1002/maco.200690031)
25. S. T. Vagge, V. S. Raja, R. G Narayanan, *Appl. Surf. Sci*. **253** (2007) 8415 (http://dx.doi.org/10.1016/j.apsusc.2007.04.045)
26. X. G. Zhang, *Corrosion and Electrochemistry of Zinc*, Plenum Press, New York, 1996 (http://dx.doi.org/10.1007/978-1-4757-9877-7)
27. M. M. Abou-Krisha, H. M. Rageh, E. A. Matter, *Surf. Coat. Technol*. **202** (2008) 3739 (http://dx.doi.org/10.1016/j.surfcoat.2008.01.015).